

# Strain Sensing Fabric for Hand Posture and Gesture Monitoring

Federico Lorussi, Enzo Pasquale Scilingo, Mario Tesconi, Alessandro Tognetti, and Danilo De Rossi

**Abstract**—In this paper, we report on a new technology used to implement strain sensors to be integrated in usual garments. A particular conductive mixture based on commercial products is realized and directly spread over a piece of fabric, which shows, after the treatment, piezoresistive properties, i.e., a change in resistance when it is strained. This property is exploited to realize sensorized garments such as gloves, leotards, and seat covers capable of reconstructing and monitoring body shape, posture, and gesture. In general, this technology is a good candidate for adherent wearable systems with excellent mechanical coupling with body surface.

Here, we mainly focused on a sensorized glove able to detect posture and movements of the fingers. It could be used in several fields of application. We report on experimental results of a sensorized glove used as movements recorder for rehabilitation therapies and medicine. Furthermore, we describe a dedicated methodology used to read the output sensors which allowed to avoid using metallic wires for the connections. The price to be paid for all these advantages is a nonlinear electric response of the fabric sensor and a too long settling time, that in principle, make these sensors not suitable for real-time applications. Here we propose a hardware and computational solution to overcome this limitation.

**Index Terms**—Biomechanics, fabric sensor, sensorized glove.

## I. INTRODUCTION

**I**N BIOLOGICAL systems, the intrinsic noisy, sloppy, and poorly selective characteristics of individual mechanoreceptors are mainly compensated by redundant allocation, powerful peripheral processing, and effective and continuous calibration through supervised and unsupervised learning and training [1]–[3], [16]. A truly biomimetic sensing system should have these features to some extent, not just as a mimicking exercise, but as a result of solid engineering reasoning [4]. Here, we report on an attempt of realizing a biomimetic sensing glove. In the literature, several studies are focused on realizing electric devices integrated into textile structure, guaranteeing hence a high wearability [5]–[7]. Here, we will describe an innovative sensorized textile technology. The lightness and the adherence of the fabric make the sensorized garments unobtrusive and uncumbersome, and hence comfortable for the subject wearing them. Moreover, the use of conventional sensors to evaluate

the posture of the hand requires the application of complicated and uncomfortable mechanical plugs in order to interface the garment with the sensors. We have chosen to realize a glove made of Lycra which satisfies the requirements of lightness, elasticity, and adherence. The new technology used to implement sensors to be integrated in usual garments is based on a conductive mixture directly spread over the fabric. This mixture does not change the mechanical properties of the fabric and maintains the wearability of the garment. It is made of commercial products, available on the market, and confers to the fabric piezoresistive properties, i.e., when the fabric is stretched, the fabric sensor shows a change in resistance. In the literature, the piezoresistivity exhibited by electrically conductive elastomer composites is statically described by using percolation theory [8]. This property is exploited to realize sensorized garments such as gloves, leotards, seat covers, and related artifacts capable of reconstructing and monitoring body shape, posture, and gesture [9]. This technology is a good candidate for adherent wearable systems with excellent mechanical matching with body surface. Here, we will describe a sensorized glove able to detect the movements of the fingers exploiting this new technology. Moreover, we will report on a dedicated topological configuration adopted to avoid using metallic wires for the connections. In spite of all these advantages, the electrical response of the fabric sensor is nonlinear and exhibits a too long settling time, that, in principle, makes these sensors not suitable for real-time applications. Here we propose a hardware solution to shorten the transient time of the sensor.

## II. MATERIALS AND METHODS

The mixture used to realize the sensors is produced by WACKER Ltd (ELASTOSIL LR 3162 A/B) and is available on the market. WACKER Ltd guarantees that the material is not toxic: “Postcured parts can be used for applications in the pharmaceutical and food industries and comply with the recommendations “XV. Silicone” of the BgVV and FDA 177.2600.” Treated fabrics have been preliminarily characterized in terms of their electromechanical transduction properties (in Fig. 3 the gauge factor  $Gf = (R - R_0)L_0 / (L - L_0)R_0$  is reported), thermal transduction properties and aging [4]. To obtain a sensorized fabric, the ELASTOSIL mixture is spread over fabric previously covered by an adhesive mask cut by a laser milling machine. The mask is designed according to the shape and the dimension desired for sensors and wires. Indeed, the empty spaces of the mask, after smearing the solution, leave suitable tracks after removing the mask. Afterwards, the fabric is put in an oven at temperature of about 130 °C for 10 min.

Manuscript received May 12, 2004; revised January 6, 2005, and April 13, 2005. This work was supported by the Defense Advanced Research Projects Agency (DARPA) and the Office of Naval Research, International Field Office (ONR-IFO) through NICOP grant N00014-01-1-0280, Pr N 01PR04487-00, and the EU Commission under Contract IST-507816 My Heart.

The authors are with the Interdepartmental Research Center “E. Piaggio”, University of Pisa, 56126 Pisa, Italy (e-mail: f.lorussi@ing.unipi.it; e.scilingo@ing.unipi.it; tescio@tiscali.it; a.tognetti@ing.unipi.it; d.derossi@ing.unipi.it).

Digital Object Identifier 10.1109/TITB.2005.854510

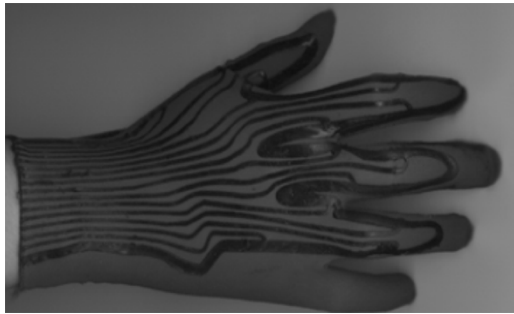


Fig. 1. Sensorized glove.

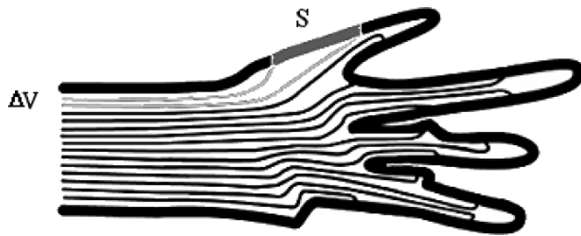


Fig. 2. Galley proof used to print the conductive mixture on the fabric glove. The black bold track represents the set of sensors connected in series, while the thin tracks represent the connection between the sensor (S) and the electronic acquisition system.

### A. Sensorized Glove

Sensing fabrics above described can be employed to realize wearable clothes able to record human posture and gesture, which could be worn for a long time with no discomfort. A suitable mask was used to print over a Lycra glove (see Fig. 1) a set of sensors and wires. In order to use the same conductive mixture of carbon-filled silicone rubber for both sensors and electric wires, a dedicated topology was used. In this way, no conventional and cumbersome cables are necessary to connect the sensors from the glove to external electronics. This configuration is the evolution of an earlier prototype where the connections between sensors and acquisition device were realized by means of metallic wires, which, inevitably, bounded certain movements. As shown in Fig. 2, the bold black track represents the set of sensors connected in series and covers the most important joints of the fingers. The thin tracks represent the connection between sensors and the electronic acquisition system. Since, as already said, thin tracks are performed by the same mixture of the main sensors, they undergo a nonnegligible change in resistance when the fingers move, but the electronic unit is designed to skip this variation. Indeed, the bold black track is supplied by a constant current. In this way, thin tracks play just the role of acquiring the voltage drop of an element of the series of sensors. On the other hand, thin tracks are connected to an instrumentation differential amplifier with high input impedance, implying that a negligible electric current flows through them. The only recorded voltage drop, therefore, refers to the sensor placed on the bold black track. Thin tracks perfectly substitute for the traditional metallic wires and behave accurately as a probe. Practically, a sensor consists in segments of the bold track between two consecutive thin tracks (the line marked as S in Fig. 2). The price to pay for all the advantages deriving from this novel technology with respect to conventional

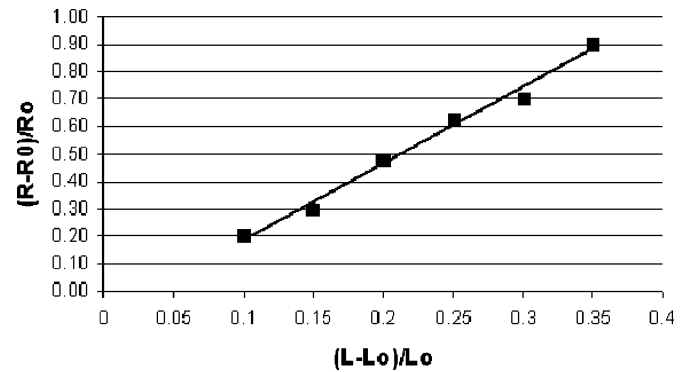


Fig. 3. Behavior of the relative variation of resistance of sensor against the relative strain.

sensing gloves is the slow nonlinear response of the sensor. In this paper, we propose a solution to this limitation, in terms of hardware and computational approach, which allowed to realize an effective and universal glove which works regardless of the size of the hand of the subject wearing it.

### III. SENSOR CHARACTERIZATION

In order to know how the fabric sensor responds to external mechanical stimuli, a suitable electromechanical characterization has been performed. A dedicated system consisting in a dc motor endowed with sensors has been designed and realized. This experimental session has been done on samples of sensors extracted from the same sensorized piece of fabric used for manufacturing the glove. A quasi-static characterization has been easily obtained by stretching several samples of fabric up to a predetermined set of lengths. In Fig. 3, the behavior of relative change in resistance against the strain is reported. The slope of the linear interpolation of the data is a rough approximation of the gauge factor. Results state that  $Gf$  depends on the shape of the printed sensors and changes with the percentage of the components of the conductive mixture and trichloroethylene.

Hereafter we will refer to sensors obtained by mixing three equal parts of the two Wackers' components and the third one of trichloroethylene. By using this mixture we have printed galley proofs 5 mm wide. The resistance obtained when the sample is unstretched, i.e., rest condition, is about 1 k $\Omega$  per cm and the gauge factor is about 2.8 (before saturation that occurs for displacement greater than 40%). The temperature coefficient of resistance (TCR), i.e.,  $TCR = ((R_T - R_{T_0})/R_{T_0})(1/(T - T_0))$ , where  $R_T$  and  $R_{T_0}$  are, respectively, the resistance at temperature  $T$  and the resistance at reference temperature  $T_0$ , is about 0.08 K $^{-1}$ . The electric impedance of smeared sensors has been measured over a frequency range 0–10 MHz and it showed neither capacitive nor inductive features, but only purely resistive behavior. In order to investigate on the dynamical characterization in terms of sensor electrical resistance versus strain, several stimuli having different waveforms were applied to the fabric sensors. When a square wave is applied as mechanical input (see Fig. 4), fabric sensor resistance increases up to a certain value (against the rise edge), then it decreases to a steady-state value. Unfortunately, this relaxing time is too long to make fabric sensors suitable for monitoring real-time human body movements.

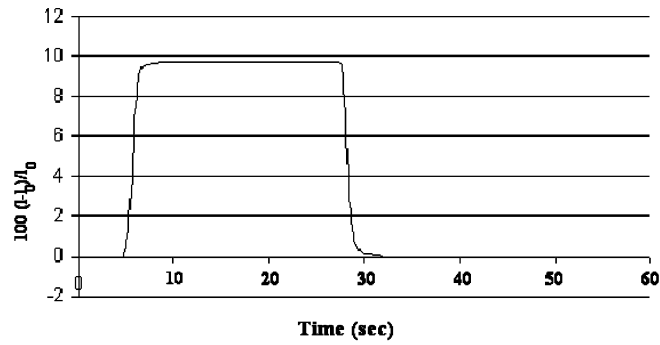


Fig. 4. Response of the fabric sensor excited by a square-wise input.

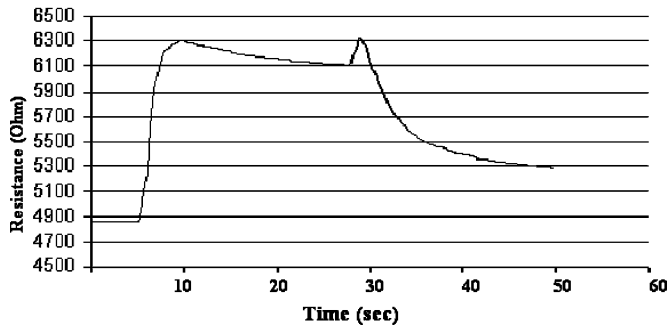
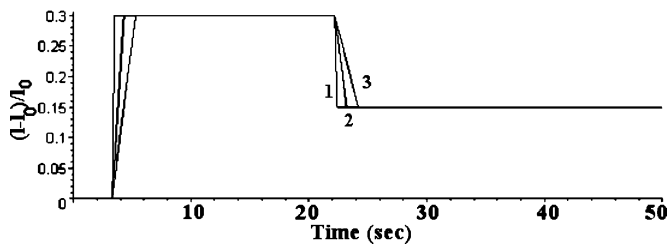


Fig. 5. Trapezoidal inputs with increasing slopes, marked with increasing numbers as well.



It is worthwhile noting in Fig. 4 that, when a decreasing step-wise input is applied, the resistance shows a little positive peak before decreasing to the settling value. This phenomenon is evident when the slope of the input signal which represents the length versus time (i.e., the strength velocity) is greater than a certain threshold. In Fig. 5 several different trapezoidal inputs (length versus time) with different slopes are reported, and in Fig. 6 the corresponding responses of the sensor are plotted. The final value of the trapezoidal signal is intentionally different from the initial one, without lacking in validity.

#### A. Model Formulation

In order to formulate a model for the sensor behavior, we have split the calculation into two different parts. The first one aims at characterizing the two peaks during the intervals with  $dl/dt \neq 0$ , while the second one at describing the transient time when  $dl/dt = 0$  (where  $l$  is the length of the sample). According to Fig. 6 we have supposed that the response of sensor depends on the velocity  $dl/dt$ . In addition, since peaks presented by the signal are always positive, even when the step-wise input is decreasing induced us to formulate a nonlinear pre-elaboration of

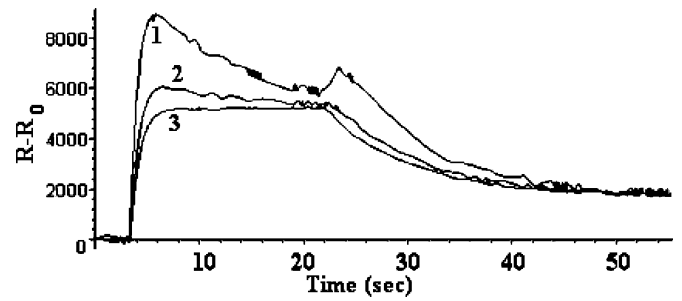


Fig. 6. Responses of the sensor to trapezoidal inputs with increasing slopes marked with corresponding increasing numbers.

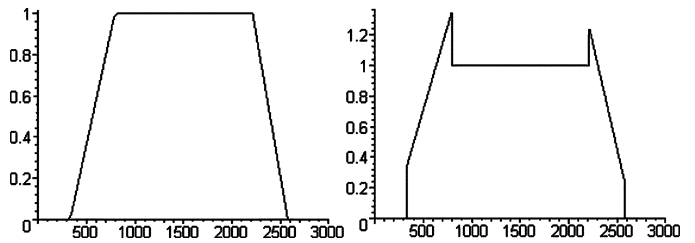


Fig. 7. Output simulation  $g(t)$  (on the right side) from the model proposed in the relationship 1 when the input signal  $l(t)$  is the trapezoidal signal depicted on the left side.

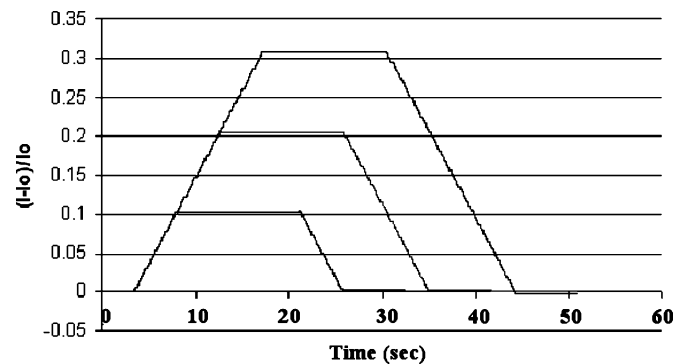


Fig. 8. Trapezoidal signals with increasing amplitude and same slope.

the inputs. This nonlinear behavior suggested us to choose an approximation containing a square component. Let us consider

$$g(t) = a_1 l(t) + a_2 \frac{dl(t)}{dt} + a_3 \frac{dl(t)^2}{dt} \quad (1)$$

where  $a_1, a_2$ , and  $a_3$  are three nonzero real numbers. This simple transformation of the inputs has given good results in modeling the sensor behavior. Fixed  $a_1, a_2$ , and  $a_3$ , for a trapezoidal input  $l(t)$ ,  $g(t)$  shows two typical peaks (as reported in Fig. 7).

After this first qualitative analysis, we performed a careful study of the experimental outputs produced by trapezoidal inputs  $l(t)$ , having increasing amplitude and same slope (see Fig. 8). Experimental data were averaged on results obtained from three tests repeated five times for each slope, obtaining a grand total of 15 trials.

The slope of the trapezoidal signals was large enough to considerably generate the two peaks. The obtained responses are plotted in Fig. 9.

By comparing Fig. 8 and Fig. 9 we can claim that when the input is kept constant after stretching, the response starts re-

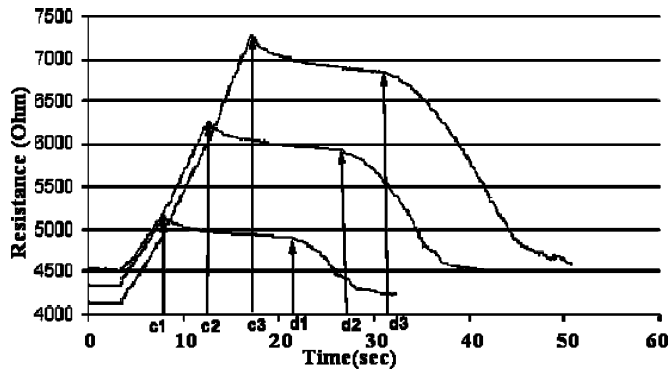


Fig. 9. Responses to trapezoidal signals with same slope.

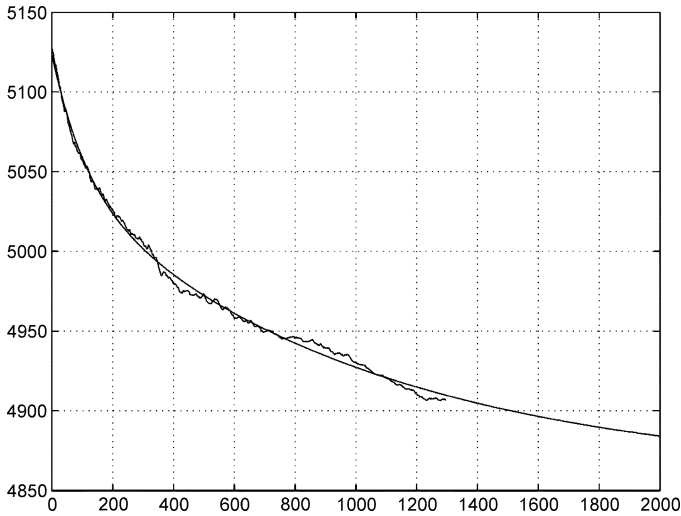


Fig. 10. Two-pole regression on decreasing step of 10% of strain.

laxing (at the points  $c_1$ ,  $c_2$ , and  $c_3$ ). According to our hypothesis (relationship 1) trends of the three signals in intervals  $[c_1, d_1]$ ,  $[c_2, d_2]$ , and  $[c_3, d_3]$  represent the transient time after the peak. These behaviors have been interpolated through an exponential regression. First, we tried to model the relaxation responses of the sensors with a one-pole differential system, but results from the regression obtained in this way were not very satisfactory. In order to improve the model performance and achieve better results, we have extended the regression to a two-pole system, by considering

$$y(t) = c_0 + c_1 e^{\omega_1 t} + c_2 e^{\omega_2 t}. \quad (2)$$

Figs. 10–12 depict to the two-poles interpolation for 10%, 20%, and 30% of strain, respectively. The estimated poles by means of this interpolation are the same for all the tests carried out and their values belong to the ranges

$$\omega_1 \in [0.06 \text{ Hz}, 0.08 \text{ Hz}] \quad \omega_2 \in [0.61 \text{ Hz}, 0.74 \text{ Hz}]. \quad (3)$$

After having calculated the pole values, we have merged the information in the classical formula of second-order linear systems. Let us consider

$$\begin{bmatrix} \dot{R} \\ R \end{bmatrix} = e^{\mathbf{A}(t-t_0)} \begin{bmatrix} \dot{R}(t_0) \\ R(t_0) \end{bmatrix} + \int_{t_0}^t e^{\mathbf{A}(t-\tau)} \begin{bmatrix} 0 \\ g(\tau) \end{bmatrix} d\tau \quad (4)$$

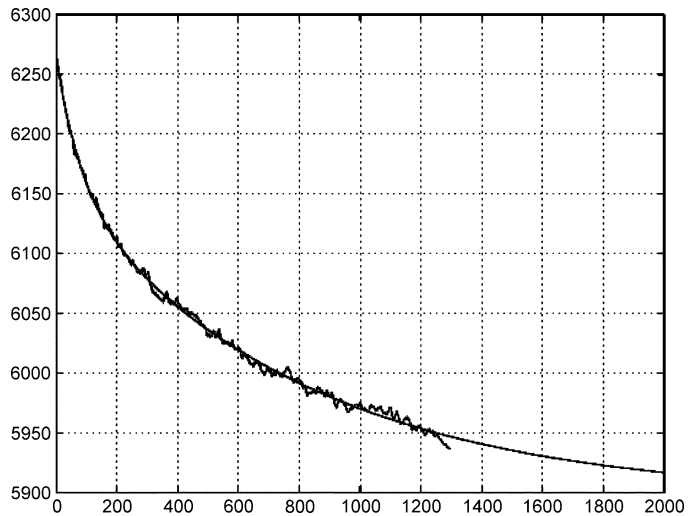


Fig. 11. Two-pole regression on decreasing step of 20% of strain.

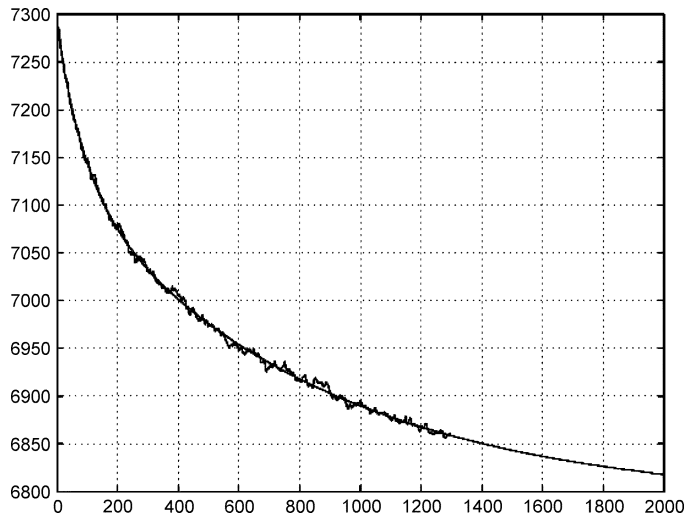


Fig. 12. Two-pole regression on decreasing step of 30% of strain.

where  $A$  is the matrix whose elements are the coefficients of the characteristic equation of the system

$$A = \begin{bmatrix} 0 & 1 \\ -\omega_1 \omega_2 & -(\omega_1 + \omega_2) \end{bmatrix}. \quad (5)$$

By simplifying (4) and considering only the second row, we obtain the expression of  $R(t)$  with respect to the three parameters  $a_1$ ,  $a_2$ , and  $a_3$ . These three parameters have been identified through the values of peaks excursions in the responses of the sensor reported in Fig. 9.

In order to assess the expression 4 with the estimated parameters, we have simulated the behavior of the system when the input of Fig. 4 is applied. What we obtain is very encouraging and is reported in Fig. 13. It is worthwhile noting that the simulation is very similar to the experimental response of the sensor (lower side of Fig. 4). Since our goal was to determine  $l(t)$  by acquiring the response of a sensor, let us derive (4) with respect to  $t$ . We obtain

$$\dot{x} = A e^{\mathbf{A}(t-t_0)} \mathbf{x}_0 + \mathbf{A} \int_{t_0}^t e^{\mathbf{A}(t-\tau)} \begin{bmatrix} 0 \\ g(\tau) \end{bmatrix} d\tau + \begin{bmatrix} 0 \\ g(t) \end{bmatrix} \quad (6)$$

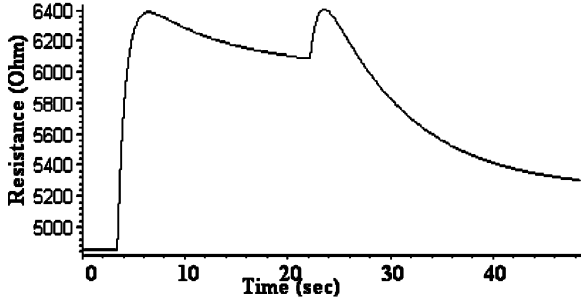


Fig. 13. Simulated output of the system when the input is a square wave, such as reported in the upper side of Fig. 4.

where  $x = [R \dot{R}]^T$  and  $x_0 = [R(t_0) \dot{R}(t_0)]^T$ . Then, by replacing (4) in (6) we get

$$\dot{x} = Ax + \begin{bmatrix} 0 \\ g(t) \end{bmatrix}. \quad (7)$$

By extracting the second row from 7, we obtain

$$[\dot{x} - Ax]_2 = g(t). \quad (8)$$

The left-hand side of (8) is known by reading the signals coming from the sensor and by using the estimated poles from the preliminary interpolation of the sensor responses. Hence, we are able to know the function  $g(t)$ . By using relationship 1, we can write the following differential equation to be computed:

$$\begin{cases} a_1 l(t) + a_2 \frac{dl(t)}{dt} + a_3 \frac{d^2 l(t)}{dt^2} = g(t) \\ l(0) = l_0 \\ \frac{dl(0)}{dt} = \dot{l}_0. \end{cases} \quad (9)$$

This equation can be dynamically solved by using as boundary conditions, at every turn, the last values of  $l(t)$  and  $\dot{l}(t)$  calculated at the previous step. Since (9) does not admit an analytical solution, it has to be integrated by using a numerical method. In Fig. 14, the solution of the differential equation (9) is given for  $R(t)$  as in Fig. 4 by using the Runge-Kutta algorithm.

Equation (9) has been processed off-line. The next developments aim at implementing it in real time. In this paper, we focused only on stationary states, i.e., when  $g(t) = a_1 l(t)$ . When the fabric sensor is submitted to an external mechanical solicitation and then it is kept still, its electrical resistance changes over time and it relaxes at the settling value. But, as shown in Fig. 4, the relaxing time of the sensor response, when submitted to a mechanical stretching, is too long to be used in real-time applications. Therefore, we focused our efforts to estimate the final value of the sensor as fast as possible. Let us consider (2) and apply the first and second derivative. Our goal is to predict the final value  $c_0$ , cancelling somehow the exponential terms. The mathematical approach to do this was to equal a linear combination of the signal, first and second derivative to a constant. Thus, we obtain

$$a(c_0 + c_1 e^{\omega_1 t} + c_2 e^{\omega_2 t}) + b(-c_1 \omega_1 e^{-\omega_1 t} - c_2 \omega_2 e^{-\omega_2 t}) + c(c_1 \omega_1^2 e^{-\omega_1 t} + c_2 \omega_2^2 e^{-\omega_2 t}) = c_0. \quad (10)$$

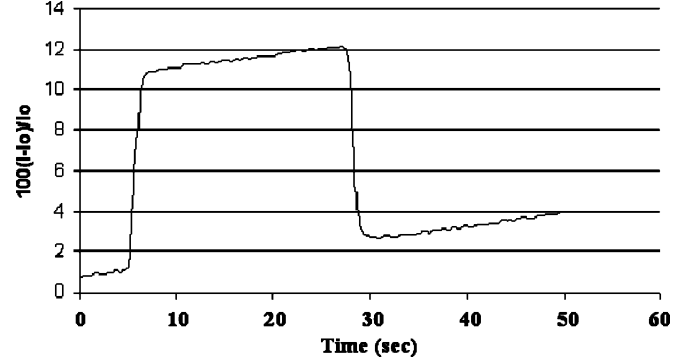


Fig. 14. Estimated input for sensor response represented in Fig. 4.

From (10), we get the following system:

$$\begin{cases} ac_0 = c_0 \\ a - b\omega_1 + c\omega_1^2 = 0 \\ a - b\omega_2 + c\omega_2^2 = 0. \end{cases} \quad (11)$$

We have three equations and three unknowns. This system is univocally determined and the solution is

$$\begin{cases} a = 1 \\ b = \frac{1+c\omega_1^2}{\omega_1} \\ c = \frac{\omega_2 - \omega_1}{\omega_1 \omega_2^2 - \omega_1^2 \omega_2}. \end{cases} \quad (12)$$

By substituting these constants in (10), we directly obtain the final value of the sensor. By summarizing, by knowing the poles of the sensor and preliminarily calculating the coefficients of the above linear combination, we are able to detect in advance the final value of the sensor skipping the too long relaxation time. Prior to using the sensor, it is necessary to perform a calibration phase in order to evaluate the poles and estimate the coefficients of the equation array (12). The detection of the regime value has been obtained via hardware by designing a suitable electronic card. In Fig. 15, the block diagram of the principle scheme is reported.

The signal from the fabric sensor is acquired and split into three lines. The first one is multiplied by the amplification gain  $a$ , the second one is differentiated and amplified by  $b$ , and the third line is differentiated twice and multiplied by  $c$ . After amplifying, the three lines go to an adder, whose output is the regime value of the relaxing response of the sensor.

In Fig. 16 is reported the output of the scheme described above compared with the response of the sensor. The sensor was submitted to a sequence of three square waves having different amplitude. It is clear from Fig. 16 that the processed response is able to shortly predict the regime value of the sensor.

## IV. APPLICATIONS

### A. The Sensing Glove as Posture and Movements Recorder

The model here proposed and above discussed has been applied to a sensorized glove. When the glove is worn by a hand which holds a certain position, the series of sensors assumes a set of values strictly related to the position. If the number of sensors is large enough, the values presented are unique for the position considered. The glove showed good capabilities of repeatability, even if it is removed from the hand and worn again

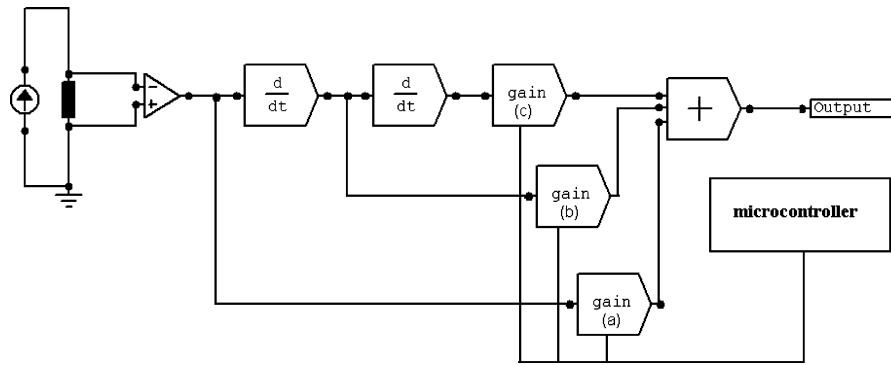


Fig. 15. Block diagram of the system for detecting the final value of the response of the sensor submitted to a stepwise stretching.

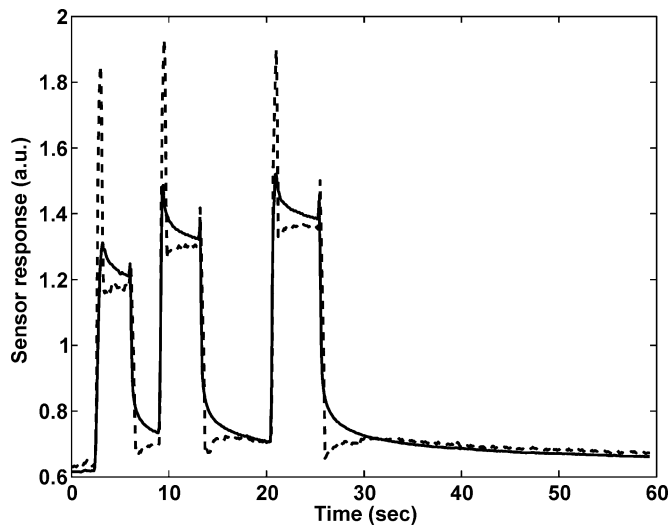


Fig. 16. Comparison between the response of the sensor (continuous curve) and the output of the conditioning system (dashed curve) able to skip the transient time.

(by the same subject). In this way, it is possible to distinguish between to different postures which can be univocally coded. We have tested this capability on a set of functionally relevant postures, the basic hand grip. A dedicated software able to recognize different postures has been implemented. Identifying only the static posture of the hand could be very simple, but it is also very promising for several applications in rehabilitation therapies and medicine. In particular, a candidate field of application is the support of a post-course of surgical operation implying an implant of a neural electrostimulator whose electrodes are positioned on nerves, directly. The operation is aimed at recovering some pre-defined basic functional grasps in a tetraplegic patient and the glove is used in different phases. In the pre-implant phase, the glove can monitor the range of grip generated by the stimulator. These grips are, hence, recorded and stored. During the surgical operation, it is necessary to verify the range of the stimulus obtained during the preparation of the implant. After positioning the electrodes adequately, by activating the neuroprosthesis, a control is performed through a suitable memory connected to the glove to verify that the gesture obtained is the same as that set up in the pre-implant phase. In the post-implant period, it is also possible to use the glove extemporaneously to



Fig. 17. Sensing glove and the electrogoniometers for the calibration phase.

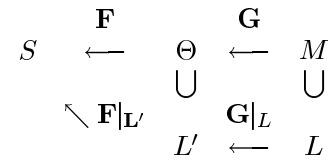
recalibrate the hardware (stimulator). The smallest deviation in posture accurately detectable by the sensing glove is  $4^\circ$ , which is an acceptable resolution in monitoring recovery of hand functionality of subjects underwent a surgical operation implying an implant of a neural electrostimulator. As an example, let us suppose of bending the metacarpo-phalangeal joint by  $90^\circ$ . We experimentally measured that fabric sensor located at this joint is stretched by 2.4 cm. Assuming a reasonable rough linear relationship between the sensor length and the joint angle, we can state that a deviation of  $4^\circ$  in the angle produces a variation of 1mm in length, i.e., 0.05 strain, being the initial length of the sensor about 2 cm. Multiplying this value of strain by the gauge factor (2.8), we obtain 0.14, which if multiplied by the initial resistance (about 1 k $\Omega$ ) we get a variation in electrical resistance of 140  $\Omega$ , easily and accurately detectable by our hardware.

Some of the basic positions acquired during the posture recorder mode can be used to construct a continuous function which maps positions into sensor values. This map, obtained as an interpolation of the discrete function which recognizes recorded posture, can be used to detect any position of the hand, even if it has never been held. Indeed, the identification algorithm is able to construct a model of the hand expressed in terms of sensor values. If the basic recorded positions are associate to a set of angle deviations for the joints of the hand, by means of a set of electrogoniometers (see Fig. 17), the inversion algorithm is able to reconstruct positions (in terms of angles) which never have been assumed by the subject.

First, let us make some considerations on what determination of human posture means by using these wearable sensors and how sensor networks can be employed. To define formally

a posture, it is necessary to develop a physical model for the particular subject holding it. We attribute a certain number of cartesian frames, one for each considered degree of freedom. In this sense, a posture is simply the set of the mutual positions with respect to the fixed frames. Obviously, the entire set of the mutual positions is not necessary to reconstruct a posture exactly, and a minimal set can be chosen in many different ways. The Denavit–Hartenberg formalism [10], for example, fixes exactly the number of relationships between frames and gives a standard method to write these positions in terms of rotation and translation affinities, for rotational and translational joints. In the case that the topological structure of the kinematic chain under study cannot be linearly approximated, it is still possible to define a model by using more sophisticated nonlinear approaches, [11], to describe the kinematics more accurately. In particular, for the kinesiology of the hand, we refer to [12] and [13], while the model for the finger kinematic chains is substantially reported in [14]. The problem can be formalized as follows. Let us assume a fixed state space (described by a set of frames assigned and by their mutual coordinate transformations) which we will designate as the posture space  $\Theta$  and which admits a well-defined topological model. To survey posture it is necessary to construct a metric on this space and then to relate the elements of  $\Theta$  to the electrical sensor configurations that span the space  $S$  of sensor readings. It is assumed that they are able to detect a variation in subject's posture and that there exists an invertible function  $\mathbf{F}$  that maps the space of the postures into  $S$ . As a consequence, the image of  $\Theta$  through  $\mathbf{F}$  is a subset of  $S$  which has the same dimension of  $\Theta$  itself. Therefore, the inverse of  $\mathbf{F}$  can be used to infer the posture from the electrical readings. The construction of  $\mathbf{F}$ , or “system identification,” is the crucial point of the method, and it is important from several points of view. It is worth pointing out that this phase is not a single sensor calibration, but a real identification of the entire system. In fact, for several reasons (the most important being the variability of body structure of the subject), the sensor location is not precisely known. However, adopting the described approach, this is no longer essential, neither is the map relating the size of a particular sensor to its electrical resistance. To better explain this point, one should consider that adherence of a sensorized fabric to the subject gives rise to intrinsic cross talk phenomena, due to the nature of the textile on which sensor are positioned. This fact, instead of being an inconvenience, is instrumental to the method we have developed, and ensures the possibility of reconstructing posture without the knowledge of the location of every single sensor. The identification concerns not only the set of sensors, but also the body structure of the subject. The same garment can be then used, in principle, to detect the posture of many different subjects with the prescribed accuracy, shifting all the variability on a different function  $\mathbf{F}$ . Metric introduction in the space of postures is realized simultaneously with the construction of  $\mathbf{F}$ . The basic idea is to relate information originating from a conventional measurement system (set of electrogoniometers, in this case) to the electrical state of a set of sensors. The former is obtained for a set of postures suitably chosen according to the topological structure of  $\Theta$ . This care is necessary because the space  $\Theta$ , related to anatomical variables

such as bones and joint positions, is not directly accessible to the observer.



Then a third space  $M$  (called “space of the markers”) is introduced with its own coordinate frame, endowed with the same topology of  $\Theta$  and of the property of effectiveness, meaning that it is always possible to determine whether two points in  $M$  coincide or not. Let us call  $\mathbf{G}$  the continuous bijective function mapping  $\Theta$  into  $M$ . Due to the effectiveness property,  $M$  has the advantage, with respect to  $\Theta$ , of being directly accessible. Let us now fix a system of coordinates and a metric in  $M$ , if  $\mathbf{G}$  is differentiable, a metric is automatically induced also on  $\Theta$ . If now a lattice  $L$ , that is a finite discrete set of points, is chosen in  $M$ , then another lattice  $L'$  in  $\Theta$  is uniquely identified via the map  $\mathbf{G}$ , and a metric is induced accordingly. Determining the law of correspondence between the lattice  $L$  and the corresponding subset of the space  $S$  means knowing the restriction of  $\mathbf{F}$  on  $L'$ . The next step is to expand the knowledge of  $\mathbf{F}$  from this restriction to all  $\Theta$ , obtaining  $\mathbf{F}$ . This is a problem of multivariate interpolation that will be discussed in the next section.

1) *Interpolation Technique AD Inversion:* In order to reconstruct position and movements not included in  $L'$ , a multivariate interpolation of  $\mathbf{F}$ , component by component has been employed. To approach this problem a piecewise linear (PL) interpolation can be performed, either directly on  $\mathbf{F}$  or on one among its pseudo-inverses. We chose the direct approach because of complexity issues that will be clarified in the following. In the direct case, we want to determine a class of linear applications from  $\Theta \rightarrow R$ , each one holding on a certain subset of  $\Theta$ . The union of these subsets must contain  $\Theta$  and the functions corresponding to adjacent subsets must coincide on their intersection. Due to the analyticity of linear applications, it is clear that two of these subsets can intersect only at their borders. The most time-consuming part of the algorithm is the partitioning of an  $n$ -hypercube whose vertices belong to  $L'$ . In order to solve the linear problem of interpolating a function defined on a given lattice (assumed to be, i.e., homeomorphic to  $Z^n$ , where  $n$  is the dimension of the space of the postures), a partitioning in  $O(n!)$  hyper-tetrahedra is necessary. Using this partitioning, the interpolation is given by finding  $O(n!)$  hyper-planes passing each one through  $n + 1$  points, representing the vertices of each hyper-tetrahedron.

Let us now prove that this partitioning exists and it is minimal by induction on the dimension of  $\Theta$ . We may suppose, without loss of generality, that the hypercube we have to subdivide is the set

$$I_n = [0, 1]^n \quad (13)$$

and let suppose that any other hypercube isometric to

$$I_{n-1} = [0, 1]^{n-1} \quad (14)$$

admits a hyper-tetrahedral decomposition. To prove that if  $I_{n-1}$  admits a decomposition, then each isometric hyper-tetrahedral of order  $n - 1$  is decomposable is trivial. Let us suppose that

$$T_{n-1} = \{t_1, \dots, t_{(n-1)!}\} \quad (15)$$

is a decomposition for  $I_{n-1}$ . Since the  $2^n$  faces of  $T_n$  are hypercubes isometric to  $I_{n-1}$ , we can suppose that all the faces of  $T_n$

$$\begin{aligned} T_{n-1}^1 &= \{t_1^1, \dots, t_{(n-1)!}^1\} \\ &\vdots \\ T_{n-1}^{2n} &= \{t_1^{2n}, \dots, t_{(n-1)!}^{2n}\} \end{aligned} \quad (16)$$

are divided in hyper-tetrahedra. Let us now consider a point  $P_n \in (0, 1)^n$ . Since  $P_n$  does not lie on any  $t_j^i$  for  $i \in \{1 \dots 2n\}$  and  $j \in \{1 \dots (n-1)!\}$ , the convex hull of the set  $\{P_n, t_j^i\}$  for  $i \in \{1 \dots 2n\}$  and  $j \in \{1 \dots (n-1)!\}$  is an  $n$ -hyper-tetrahedron. Let consider now the set of all hyper-tetrahedra obtained in this way

$$T^* = \{CH(\{P_n, t_j^i\}) \mid i \in \{1 \dots 2n\}, j \in \{1 \dots (n-1)!\}\} \quad (17)$$

where  $CH$  is the function which computes the convex hull. The cardinality of  $T^*$  is exactly  $2n(n-1)! = 2n!$ . Moreover, two hyper-tetrahedra  $CH(\{P_n, t_{j_1}^{i_1}\})$  and  $CH(\{P_n, t_{j_2}^{i_2}\})$  can intersect only on their borders, otherwise  $t_{j_1}^{i_1}$  and  $t_{j_2}^{i_2}$  would intersect on their internal parts (precisely on the projection from  $P_n$  to  $t_{j_1}^{i_1}$  and  $t_{j_2}^{i_2}$ ). Let us now note that if we move  $P_n$  on a face of  $I_n$ , the number of the nontrivial hyper-tetrahedra in  $T^* = T_{-1}^*$  reduces to  $2n(n-1)! - (n-1)!$ , if  $P_n$  lies on the intersection of two faces on  $I_n$ , the cardinality of  $T^* = T_{-2}^*$  reduces to  $2n(n-1)! - 2(n-1)!$  and so on. In particular, if  $P_n$  lies on the intersection of  $n$  faces of  $I_n$ , then  $T^* = T_{-n}^* = T_n$  and its cardinality is equal to  $2n(n-1)! - n(n-1)! = n(n-1)! = n!$ . For the first step, consider a square which represents a 2-hypercube and which is trivially divided into two triangles. *Ad absurdum*, let us suppose that  $I_n$  admits a decomposition of cardinality smaller than  $n!$ . By repeating all the procedures executed to construct the partition, we will obtain that a square is divisible into a single triangle. From the existence of the partition, a recursive procedure to construct it can be implemented for each hypercube of the lattice. When a partition is computed for all the hypercubes, interpolating each sensor is equivalent to solving  $n_l(n!)$  (algebraic) linear systems in order to determine the equations of the hyperplanes (where  $n_l$  is the number of hypercube which constitute the lattice). The algorithm has an exponential complexity in the dimension of  $\Theta$ , but all this computation is done off-line. After having interpolated the functions which represent the set of sensors, and calculated the pseudo-inverse  $\mathbf{F}^\dagger$  of the function  $\mathbf{F}$  [15], we are ready to employ them to detect the posture  $\theta$  of a subject wearing the sensing glove. This procedure is executed only once. Then a new calculated map is applied to every measurement. This method is time consuming when it calculates the  $O(n!)$  pseudo-inverse. The pseudo-inverse  $\mathbf{F}^\dagger$  can be employed

to define an iterative numerical method able to reconstruct the posture of the hand. After having calculated it, an iterative algorithm starts considering an estimation  $\theta_0$  of the posture to detect and refine it by using the formula

$$\theta_{i+1} = \theta_i + k\mathbf{F}^\dagger(\mathbf{s}_{i+1} - \mathbf{s}_i) \quad (18)$$

(Newton–Rhapson).

## B. Methods

The algorithm described in the previous section is, however, devoted to recognizing static configurations of the hand, disregarding the dynamic transition from one posture to another. Twenty subjects (11 females, 9 males) volunteered to participate in the experiments. Their ages ranged from 25 to 35 years, with an average of 28.1, with a university degree and normal health conditions. All participants were naive of the purposes of the experiment. The experimental session was split into two stages. The first stage was based on the recognition of a set of standard postures of the hand against a preliminary calibration and storing of all allowed configurations, while in the second phase, the capability of the sensing glove to identify a position of the hand not included in the pre-stored set of postures was tested. In particular, in the first phase, a group of subjects were required to perform 32 well-known reproducible configurations belonging to the basic grip and the hand-shapes of American Sign Language. In the preliminary phase, volunteers were asked to perform all 32 postures and the signals from sensors were acquired and recorded. In this phase, we did not use the hardware able to jump the relaxation time, but we waited long enough to acquire the steady-state values. Afterwards, subjects were required to repeat the postures, in random order, and our system, comprised of hardware and software implementing the algorithm able to shrink the settling time, should recognize the posture.

## C. Results

The glove recognized 100% of the postures previously recorded if it was not removed from the hand, and 98% when it was worn again. The recognition percentage increased again to 100% if the subject slightly re-adjusted the glove when the first error occurs. Indeed, it was experimentally proved that the error was due to a mismatch between the glove and the hand. The second stage of the experimental session implied a preliminary identification phase with a set of different positions. Afterwards, subjects were asked to freely hold a generic posture of the hand. The electric values of the sensors were acquired by the hardware, enabling it to estimate very quickly the final values, and our algorithm discussed in the previous section was applied. Estimated postures were compared with the real ones. By way of illustration, some of these data are collected in Table I. On average, the error percentage in detecting the actual angle is about 4%. Table I reports error percentage greater than 4%, but on average we obtained this value. It is worthwhile pointing out that as the largest part of the ASL signs are realized by assuming static postures of the hand, the glove is enabled to

TABLE I

REAL ANGLE VALUES AND ESTIMATED ANGLE VALUES FOR THE METACARPO-PHALANGEAL JOINT (IN FLEXION-EXTENSION), THE PROXIMAL INTERPHALANGEAL JOINTS, AND THE DISTAL INTERPHALANGEAL JOINT OF THE FOREFINGER AT DIFFERENT TEST POINTS. THE REAL AND ESTIMATED ANGLES ARE EXPRESSED IN DEGREES. THE LAST COLUMN SHOWS THE NUMBER OF STEPS NECESSARY TO RECONSTRUCT THE VALUES

	Met-Fal	Int-proxs	Int-Dist	N° steps
<b>Real</b>	45	45	0	34
<b>Estimated</b>	45	45	0	
<b>Real</b>	45	22.5	22.5	25
<b>Estimated</b>	45	25.31	15.47	
<b>Real</b>	45	45	45	3
<b>Estimated</b>	45	42.19	45	
<b>Real</b>	75	75	25	26
<b>Estimated</b>	80.16	67.5	32.34	
<b>Real</b>	60	0	0	33
<b>Estimated</b>	60.47	0	8.44	
<b>Real</b>	22.5	22.5	22.5	17
<b>Estimated</b>	22.5	22.5	22.5	

recognize them without delay, exploiting the transient reduction algorithm. Theoretically, the algorithm is capable of detecting slow movements as well as fast movements; actually, derivative blocks amplify quick variations of signals, introducing noise into calculations. We are currently investigating a mathematical method which ensures the determination of  $g(t)$  without explicitly differentiating signals.

## V. CONCLUSION

In this paper, we reported on a sensorized glove realized by using a new technology based on fabric sensors. In the first part of the paper, the dynamical behavior of the sensor was analyzed. The single fabric sensor has been modeled as a second-order system. Since the response of the sensor is nonlinear, a linearization preprocessing has been applied. By means of an exponential regression, the relaxing part of the sensor response has been interpolated and the poles of the system have been identified. By knowing the poles of the system and the value of the output of the sensor, it is possible to extrapolate the input applied. This inversion algorithm has been proposed and solved through a numerical simulation. The next developments aim at solving this algorithm in real time. In the meantime, we focused on the stationary states of the sensor response, i.e., we identified the initial and final value of the sensor during a variation, skipping the transient time. We proposed a dedicated topological configuration in order to implement this methodology via hardware. Results have been very satisfactory. In order to validate and assess this methodology, it has been applied on the sensorized glove during experiments of posture detection. In particular, 32 postures including the basic grip and signs of American Sign Language were used in the evaluation phase. The results of the evaluation are quite encouraging and promising for continuing this work successfully. Indeed, when the glove was used without being removed from the hand, the American Sign Language postures

were measured with 100% accuracy. When the glove was removed and worn again, the accuracy fell only to 98%.

## ACKNOWLEDGMENT

The authors would like to thank G. Zupone for his contribution to this paper.

## REFERENCES

- [1] F. J. Clark and K. W. Horch, "Kinesthesia," in *Handbook of Perception and Human Performance*, K. R. Boff, L. Kaufman, and J. P. Thomas, Eds. New York: Wiley, 1986, pp. 1-62.
- [2] P. R. Burgess, J. Y. Wei, F. J. Clark, and J. Simon, "Signaling of kinesthetic information by peripheral sensory receptors," *Ann. Rev. Neurosci.*, vol. 5, pp. 171-187, 1982.
- [3] A. Mulder, "Human Movements Tracking Technology," Simon Fraser Univ., Sch. of Kinesiology, Burnaby, BC, Canada, Hand Centered Studies of Human Movement Project. Tech. Rep., 1994.
- [4] F. Lorussi, W. Rocchia, E. P. Scilingo, A. Tognetti, and D. De Rossi, "Wearable, redundant fabric-based sensor arrays for reconstruction of body posture," *IEEE Sensors J.*, vol. 4, no. 6, pp. 807-818, Dec. 2004.
- [5] E. R. Post, M. Orth, P. R. Russo, and N. Gershenfeld, "E-broidery: Design and fabrication of textile-based computing," *IBM Syst. J.*, vol. 39, no. 3&4, pp. 840-860, 2000.
- [6] R. V. Gregory, W. C. Kimbrell, and H. H. Kuhn, "Electrically conductive non-metallic textile coatings," *J. Coated Fabrics*, vol. 20, pp. 1-9, 1991.
- [7] E. P. Scilingo, F. Lorussi, A. Mazzoldi, and D. De Rossi, "Strain-sensing fabrics for wearable kinaesthetic-like systems," *IEEE Sensors J.*, vol. 3, no. 4, pp. 460-467, Aug. 2003.
- [8] M. Taya, W. J. Kim, and K. Ono, "Piezoresistivity of a short fiber/elastomer matrix composite," *Mech. Mater.*, vol. 28, pp. 53-59, 1998.
- [9] D. De Rossi, F. Lorussi, A. Mazzoldi, P. Orsini, and E. P. Scilingo, "Active dressware: wearable kinesthetic systems," in *Sensors and Sensing in Biology and Engineering*, F. G. Barth, J. A. C. Humphrey, and T. W. Secomb, Eds: Springer-Verlag, ch. 26, pp. 379-392.
- [10] J. Denavit and R. S. Hartenberg, "A kinematic notation for lower-pair mechanism based on matrices," *J. Appl. Mech.*, vol. 77, pp. 215-221, 1955.
- [11] D. J. Montana, "The kinematics of contact and grasp," *Int. J. Robot. Res.*, vol. 7, no. 3, pp. 17-32, 1988.
- [12] I. A. Kapandji, *Physiologie articulaire. Schémas commentés de mécanique humaine, Tome 1: Membre Supérieur*, E. M. Paris, Ed., 1999.
- [13] M. A. McConail and J. V. Basmajian, *Muscles and Movements*. New York: Krieger, 1977.
- [14] E. Y. Chao, A. Kai-Nan, and Y.-S. Chao, *Biomechanics of the Hand: A Basic Research Study*. Singapore: World Scientific, 1987.
- [15] A. Quarteroni, R. Sacco, and F. Saleri, *Numerical Mathematics*. New York: Springer, 2000.
- [16] P. M. Rack and D. R. Westbury, "The effects of length and stimulus rate on tension in the isometric cat soleus muscle," *J. Physiol.*, vol. 204, pp. 443-460, 1969.



**Federico Lorussi** graduated in mathematics and computer science from the University of Pisa, Pisa, Italy, with a thesis on the observability of nonlinear dynamical system and the applications of the Hilbert's function to the Buckberger's computer algebra algorithm on Groebner Basis. In December 2003, he received the Ph.D. degree in automation, robotics and bioengineering from the University of Pisa with a thesis on the analysis and the synthesis of human movements.

Currently, he is a Postdoctoral Researcher in the Information Engineering Department of the University of Pisa. His research is related to anthropomorphic robotics and biomechanics. He is the author of several papers, contributions to international conferences, and chapters in international books.



**Enzo Pasquale Scilingo** received the Laurea degree in electronic engineering from the University of Pisa, Pisa, Italy, and the Ph.D. degree in bioengineering from the University of Milan, Milan, Italy, in 1995 and 1998, respectively.

For two years, he was a Postdoctoral Fellow with the Italian National Research Council, and currently he is a Postdoctoral Fellow with the Information Engineering Department, University of Pisa, and he pursues his research work with the Interdepartmental Research Center "E. Piaggio." His research interests are

in haptic interfaces, biomedical and biomechanical signal processing, modeling, control, and instrumentation. He is the author of several papers, contributions to international conferences, and chapters in international books.



**Mario Tesconi** graduated in biomedical electronic engineering from the University of Pisa, Pisa, Italy, in 2001. In December 2002, he started a collaboration with the Pisa Research Centre (CPR) to manage the European research project "MEGA" regarding music performance and full-body movements as first class conveyors of expressive and emotional content. Currently, he pursuing the Ph.D. degree in automation, robotics and bioengineering.

His recent research interests are predominantly focused on lower limb biomechanics with a specific study on the design and realization of a knee sleeve able to detect the posture and movement of the knee joint.



**Alessandro Tognetti** graduated in electronic engineering from the University of Pisa, Pisa, Italy, with a thesis on the microfabrication and characterization of carbon nanotube electromechanical actuators. In December 2004, he finished the Ph.D. course in automation, robotics and bioengineering and he is currently preparing the final thesis.

His main research interests concern the design and development of wearable devices for biomechanical and multimedia application. He is currently working on the design of wearable kinesthetic interfaces devoted to human posture and movement detection with a specific focus on the

development of algorithms and software packages for data treating and processing. He is the author of several papers, contributions to international conferences, and chapters in international books.



**Danilo De Rossi** graduated from University of Genova, Genova, Italy, with the Ph.D. degree in chemical engineering in 1976.

From 1976 to 1981, he was a Researcher with the Institute of Clinical Physiology of CNR. He worked in France, USA, Brazil, and Japan. Since 1982, he has been with the School of Engineering, University of Pisa, Pisa, Italy, where presently he is a Full Professor of Bioengineering and President of the Biomedical Engineering Teaching Track. Since 1999, he has also been an Adjunct Professor of Material Science with

Wollongong University, Wollongong, Australia. His scientific activities are related to the physics of organic and polymeric materials, and to the design of sensors and actuators for bioengineering and robotics. He is the author of over 150 technical and scientific publications, and is co-author of seven books.